Review

Structural insights into gap junction channels boosted by cryo-EM

Atsunori Oshima[1, 2, ¶]

[1]Cellular and Structural Physiology Institute (CeSPI), Nagoya University, Furo-cho, Chikusa-ku, Nagoya 464-8601, Japan

[2]Department of Basic Medicinal Sciences, Graduate School of Pharmaceutical Sciences, Nagoya University, Furo-cho, Chikusa-ku, Nagoya 464-8601, Japan

¶To whom correspondence should be addressed: Atsunori Oshima

Cellular and Structural Physiology Institute (CeSPI)

Department of Basic Medicinal Sciences, Graduate School of Pharmaceutical Sciences, Nagoya University, Furo-cho, Chikusa-ku, Nagoya 464-8601, Japan

Tel: +81-52-747-6837

Fax: +81-52-747-6795

E-mail: atsu@cespi.nagoya-u.ac.jp

Short title: Cryo-EM structures of gap junction channels

Key words: gap junction channel, high-resolution structure, cryo-EM, phospholipids, N-terminal rearrangement

ABSTRACT

Regulating intercellular communication is essential for multicellular organisms. Gap junction channels are the major components mediating this function, but the molecular mechanisms underlying their opening and closing remain unclear. Single-particle cryo-electron microscopy (cryo-EM) is a powerful tool for investigating high-resolution protein structures that are difficult to crystallize, such as gap junction channels. Membrane protein structures are often determined in a detergent solubilized form, but lipid bilayers provide a near native environment for structural analysis. This review focuses on recent reports of gap junction channel structures visualized by cryo-EM. An overview of the differences observed in gap junction channel structures in the presence and absence of lipids is described, which may contribute to elucidating the regulation mechanisms of gap junction channel function.

Introduction:

Gap junction channels are critical for chemical and electrical coupling of adjacent cells. Electrical coupling of native neuronal cells was reported more than 60 years ago [1,2], and the morphology of the cellular components involved was subsequently observed by electron microscopy [3,4]. The molecular mechanisms underlying their functionality, specifically with regard to channel opening and closure, and the permselectivity and modulation by chemical compounds, however, remain unclear. Electrophysiologic studies revealed that gap junction channels exhibit characteristic gating features in response to transjunctional voltage [5], membrane potential [6], and chemical factors such as calcium and pH [reviewed in 7]. The structures of gap junction channels that account for their closure, however, are less well studied.

Two protein families are known to form gap junctions, chordate connexins and pre-chordate innexins [8]. Both protein families possess four transmembrane helices forming oligomeric structures of a hemichannel in a single membrane, and an intercellular junction channel comprising face-to-face docked hemichannels spanning two plasma membranes. Gap junction structures are historically studied using electron crystallography and X-ray crystallography [9–14]. Single-particle cryo-electron microscopy (cryo-EM), however, provides markedly improved resolution [15,16]. This method has allowed us to visualize the atomic structure of the innexin-6 (INX-6) gap junction channel [17]. The gap junction channel structures determined by electron crystallography, X-ray crystallography, and single-particle cryo-EM were summarized in a recent review [18]. Interestingly, many gap junction structures exhibit a wide pore in the open form, except for low-resolution two-dimensional crystallographic structures of Cx26M34A [11] and N-terminal deleted INX-6 [13] in a lipid bilayer. Because these structures are mutant channels, however, it remains uncertain if they correspond to physiologic closure. Two recent studies reported cryo-EM structures of gap junction channels. One was a Cx46/50 gap junction channel in amphipol isolated from sheep lens [19●●], and the other was undocked INX-6 hemichannels in a nanodisc or detergent [20●●]. The latter study provided the first high-resolution structure of a gap junction channel in phospholipids, although lipid molecules are not usually considered when elucidating

the mechanism of gap junction channel closure. In this review, updated reports on gap junction structural biology observed using cryo-EM are featured for discussing channel closure, and shedding light on the contribution of the lipid bilayer environment for elucidating channel structure.

Cryo-EM structure of Cx46/50 gap junction channels isolated from sheep eye lens

The structure of Cx46/50 determined using a cryo-EM technique was recently reported [19●●]. This was intriguing because this is a native membrane protein and not a recombinant membrane protein, and the structure comprised a mixture of two connexin isoforms, Cx46 and Cx50. Most cell types are generally considered to express multiple connexin isoforms [21], which contributes to the difficulties in solving a high-resolution structure of native gap junction channels [22]. In this cryo-EM study, the structure was determined at 3.4 Å resolution. Atomic structures of Cx46 and Cx50 were generated based on this high-resolution map along with the comparative analysis. Experimental density identified features of both models that were less well-defined by the density map at which the two isoforms differ in sequence. On the other hands, the densities of the amino acid side chains are clearly resolved where the two isoforms share a sequence. These allow for modeling of the two atomic structures of Cx46 and Cx50.

This paper also discusses the use of electrostatistic potentials to study ion permeation and selectivity. The coulombic surface potential of the Cx50 pore constriction is strongly negative (Fig. 1(A)), consistent with the lowest energy barrier for K^+ (1.4 kcal/mol), whereas the peak energy barrier to Cl^- is higher (4.8 kcal/mol). This trend is also observed for Cx46 (Fig. 1(B)) and is consistent with the high cation selectivity of Cx50 and Cx46 [23,24]. Cx26 has a weaker barrier because it has more positive residues at the cytoplasmic entrance than Cx46 and Cx50 (Fig.1(C)), and reportedly prefers cation permeation over anion permeation [25]. The surface potential becomes more complicated when Cx46 and Cx50 are mixed to form heteromeric or heterotypic channels. The uneven distribution of the coulombic surface potential may account for the rectification of Cx46/50 heterotypic channels by asymmetric free-energy landscape where Cx46 exhibits higher than Cx50 for K^+ [19●●]. The importance of the electrostatic surface potential for channel gating was implicated by the recent X-ray structures of Cx26 bound with and

without Ca^{2+} on the extracellular side of a conduit [14], but this structure does not show the arrangement of the N-terminal domain, which is considered essential for voltage-dependent gating in Cx26 and Cx32 [5,26].

Similar but distinct organization of the Cx46/50 N-terminus

The structure of Cx46/50 takes on an N-terminal funnel configuration to stabilize the open state. The X-ray structure of Cx26 is also interpreted to be an open form [12], but shows a distinct feature in terms of the arrangement of the N-terminal helix. The N-terminus of Cx46/50 is stabilized by hydrophobic anchoring between the hydrophobic faces of the N-terminus and pore-lining helices of TM1 and TM2 (Fig.2(A)) rather than the hydrogen bond network through D2 in Cx26 (Fig. 2(B)). In molecular dynamics simulations, a transient intermolecular hydrogen-bond network interaction is observed in a non-N-terminal acetylated state [19●●], similar to those observed in the Cx26 X-ray structure that does not show the densities for M1 or acetylation [12], while mass spectrometry analysis revealed that the N-terminus of Cx26 is acetylated [27]. Because Cx26 is categorized as a beta-type connexin and exhibits no compatibility for functional heteromeric channel formation with either Cx46 or Cx50 [28], which are classified as alpha type connexins. The N-terminus of Cx26 is quite flexible and dynamic as implicated by molecular dynamics simulations and NMR structural analyses [29–31], which is consistent with high temperature factor distribution in the Cx26 X-ray structure [12] (Fig. 2(C)). It is not surprising that the N-terminal arrangement and its stability are not identical between these two types of connexins. The structure of Cx46/50 in a lipid bilayer would be interesting to learn about the stability of the N-termini of Cx46/50 in a more native environment.

Structures of INX-6 gap junction hemichannels in phospholipids or detergent

The high-resolution structures of connexin and innexin gap junction channels described above are all in a detergent-solubilized form, not in the native plasma membrane. A cryo-EM structure of INX-6 in a nanodisc was recently determined at 3.8 Å resolution [20●●] (Fig. 3(A)). This structure is an undocked

hemichannel embedded in phospholipids. The extracellular surface in an undocked form is partially disordered, but rearrangement, such as in a model of loop-gating [32], is not observed. The INX-6 undocked hemichannel in detergent clearly shows an N-terminal funnel in the pore (Fig.3(B)), consistent with a docked junction form in detergent [17]. The structure in a nanodisc, however, exhibits an N-terminal conformation that differs from the pore funnel in detergent, deflecting to the cytoplasmic side, and the pore is blocked by double-layer densities (Fig. 3(A)). In comparison with the hemichannel structure of the N-terminal deleted INX-6 (Fig. 3(C)), these layer densities may be accounted for by phospholipid head groups. The INX-6 N-terminus is assumed to be flexible enough to take various conformations with different distribution probabilities in and around the pore depending on presence or absence of a lipid bilayer (Fig. 3(D)). As none of the earlier studies of gap junction channels suggested that the N-terminus is oriented to the outside of the channel, the N-terminal helix (NTH) is simply assigned on the density inside the pore. It is important to note that artifacts resulting from the nanodisc reconstitution cannot be excluded. In addition, this flexible distribution of the N-terminus may be specific to INX-6 channels, and not a general feature of connexin channels.

Characteristic features in the pore of undocked INX-6 gap junction hemichannels in phospholipids

The hemichannel structure of INX-6 reconstituted in a nanodisc is the first report of a gap junction protein in phospholipids at near atomic resolution that shows a blocked pore. While it is uncertain if this structure is physiologic, the structure in a nanodisc provides implications for interpreting the channel closure of gap junctions. There are two notable features. One feature is the N-terminal rearrangement depending on the presence and absence of phospholipids. The electrophysiology of connexins suggests that transjunctional voltage-dependent gating is initiated by the movement of an N-terminal voltage sensor [26,33]. It remains unresolved, however, how the N-terminus moves during its functional process. Simple plugging with the N-termini would allow for opening the pore when the N-terminal plug goes to the cytoplasmic side [11]. This is not very consistent with a proposed model based on functional studies that the hemichannel is closed when the N-terminus moves to the cytoplasmic side and is open when it is

located at the extracellular side in the pore [33]. If the lipid bilayer environment induces the N-terminal deflection to the cytoplasmic side, the situation becomes more complicated as the protein-lipid interaction should be incorporated into the molecular machinery.

The second feature is pore blockage by a double-layer obstruction such as a lipid bilayer. At present, the plausibility of this interpretation is tentative because it is difficult to clearly label lipid molecules in a cryo-EM map [20●●]. Alternative possibility is unresolved N-terminal portion may contribute to these pore densities. More than 10 amino acid residues are still unresolved in the structure of wild-type INX-6 in a nanodisc. Interestingly, in contrast to connexin structures, in INX-6 structures unassigned densities are usually found in the space between the transmembrane helix bundles (Fig. 3(E)) [17,20●●]. Although this space itself is not large enough for a lipid molecule like POPC (1-palmitoyl-2-oleoyl-sn-glycero-3-phosphocholine) to pass through back and forth, molecular dynamics simulations suggest that the space is still accessible for lipids [20●●]. If INX-6 can assume asymmetric conformations like the relaxed and compact forms found in the leucine-rich repeat-containing 8A (LRRC8A) channel [34●●], lipid access to the pore would be more likely. The driving force required for N-terminal rearrangement in a lipid bilayer environment, however, remains to be clarified. Studies of the open conformation structure of INX-6 in a lipid bilayer are necessary to further understand the mechanisms of closure. In addition, structure determination under membrane potential conditions would be useful to elucidate whether the movement depends on the voltage, but this would be very difficult with single particle cryo-EM as well as crystallography.

Previous works have demonstrated that the mutants of gap junction proteins with deletions or point mutations in the N-terminus often result in the loss of function [13,35–38]. These findings conflict with the notion of a simple blocking mechanism by the N-terminal helices [11,39], because the N-terminal deletion mutants, without a funnel in the pore, should have an open pore because of the wider space of the pore pathway if the pore is regulated only by the N-terminal peptides. To interpret the closure of the N-terminal deletion mutants of gap junction channels, an alternative factor other than the N-terminal domains should be considered, such as the involvement of phospholipids in the pore as implicated for

INX-6 channels. Again, it should be noted that the lipid-mediated closure and N-terminal rearrangement may be specific to INX-6 gap junction channels.

The leucine-rich repeat-containing 8 (LRRC8) protein family has homology with innexin [40,41], and members of this family are categorized as volume-regulated anion channels in a single membrane [41,42]. Recently, the LRRC8A channel was determined by cryo-EM in detergent and in a nanodisc [34●●,43–45●]. Unfortunately, the N-terminal region (amino acids 1-14) is disordered in those structures. In detergent, the two forms of LRRC8A, compact and relaxed, exhibit different amounts of space between the adjacent subunits in the transmembrane domains [34●●]. These two loose and tight interfaces may represent the regulation of the gating function of LRRC8A. In a nanodisc, however, the rearrangement between constricted and expanded states is mainly observed on the cytoplasmic side, not in the transmembrane domains [45●]. The intrinsic function in vivo differs between the LRRC8A anion channel and INX-6 gap junction channel. Nevertheless, the two distinct conformations of LRRC8A may provide insight into the tertiary structural change of other homologous proteins such as INX-6.

Phospholipid distribution in the structures of other membrane proteins

A few reports suggest that phospholipids are associated with the closure or regulation of the protein activity. An electron crystallographic study reported an unassigned density in the middle of a rotor ring of an ATP synthase [46]. This density is estimated to comprise phospholipids [47]. In the X-ray structure of the K-ring of bacterial V-ATPase, phospholipids are observed on the inside surface of the rotor ring [48]. A recent high-resolution cryo-EM structure of a V-ATPase V_o proton channel reconstituted in a nanodisc exhibited helices, not phospholipids, of Voa1 and c'' inside the rotor ring [49], indicating that the density inside the ring should be cautiously interpreted. The pore diameter of wild-type INX-6, 30 ~ 40 Å, is consistent with the rotor ring diameters of V-ATPase [48] and F_oF_1-ATP synthase [50]. These structures suggest that an occluded space of this size can be occupied by lipids or helices when oligomerized structures are embedded in the membrane.

TWIK-1, a tetrameric ion channel, shows side fenestrations that are occupied by lipid alkyl chains,

and these lipids are able to access the ion-conducting pore through the fenestrations [51]. Additionally, it has been proposed for TRAAK that lipid acyl chain access controls the gating and mechanosensitivity of the channel [52]. In the crystal structure of the NabAb, a bacterial sodium channel, the side fenestration is also speculated to be occupied by phospholipids [53]. Because these channels possess distinct functions from gap junctions, care should be taken against overestimating and extending the interpretation to gap junction channels. The contribution of lipid-protein interactions to the channel function should be considered when a difference is observed between high-resolution structures in detergent and in phospholipids as found for the INX-6 structures.

Perspective

In previous functional and structural studies of gap junctions, protein-lipid interactions have not attracted a lot of attention because of the lack of high-resolution structures reconstituted in phospholipids. This is because high-resolution structures are often studied with detergent-solubilized proteins [12,14] and two-dimensional crystallographic studies have not reached high-resolution [9–11,13]. The structure of an undocked INX-6 hemichannel in phospholipids suggests that the molecular mechanism of functionality should be interpreted in consideration of a lipid bilayer environment. As elucidated for INX-6, cryo-EM with nanodiscs would be a promising strategy for studying connexin channels. While there have been several regulatory models of gap junction activity proposed on the basis of structural and functional approaches [9,14,39,54,55], these are not well cross checked by different isoforms of connexins or innexins. To investigate membrane protein structures in their more native lipid environment, cryo-EM techniques were effectively used for two-dimensional crystals of membrane proteins embedded in lipid bilayer [56,57], and now applied to membrane proteins in nanodiscs with single particle analysis. This cutting-edge technique is necessary for elucidating the closed form of gap junction channels at high-resolution. Protein-lipid interactions may be a crucial factor for resolving the discrepancy in terms of functional models of gap junction channels.

Conflict of interest

The author declares no conflicts of interest associated with this manuscript.

Acknowledgments

I am grateful to Dr. Kazutoshi Tani (Mie Univ.) for critical reading of the manuscript. This work was supported by the Platform Project for Supporting Drug Discovery and Life Science Research (Basis for Supporting Innovative Drug Discovery and Life Science Research (BINDS)) from AMED under Grant Number JP19am0101074, and Grants-in-Aid for Scientific Research (B) under Grant Number JP19H03165.

References

[1] Furshpan, EJ, Potter DD: **Mechanism of nerve-impulse transmission at a crayfish synapse.** *Nature* 1957, **180**:342–343.

[2] Furshpan EJ, Potter DD: **Transmission at the giant motor synapses of the crayfish.** *Physiol* 1959, **145**:289-325.

[3] Bennett MVL, Aljure E, Nakajima Y, Pappas GD: **Electronic junctions between teleost spinal neurons: electrophysiology and ultrastructure.** *Science* 1963, **141**:262-264.

[4] Robertson JD: **The occurrence of a subunit pattern in the unit membranes of club endings in Mauthner cell synapses in goldfish brains.** *J Cell Biol.* 1963, **19**:201–221

[5] Verselis VK, Ginter CS, Bargiello TA: **Opposite voltage gating polarities of two closely related connexins.** *Nature* 1994, **368**:348-351.

[6] Obaid AL, Socolar SJ, Rose B: **Cell-to-cell channels with two independent regulated gates in series: analysis of junctional channel modulation by membrane potential, calcium and pH**, *J. Membr. Biol.* 1983, **73**:69–89.

[7] Peracchia, C: **Chemical gating of gap junction channels; roles of calcium, pH and calmodulin.** *Biochim. Biophys. Acta.*2004, **1662**:61-80

[8] Phelan P: **Innexins: members of an evolutionarily conserved family of gap-junction proteins.** *Biochim. Biophys. Acta*. 2005, **1711**:225-245

[9] Unwin PN, Ennis PD: **Two configurations of a channel-forming membrane protein.** *Nature* 1984, **307**:609-613.

[10] Unger VM, Kumar NM, Gilula NB, Yeager M: **Three-dimensional structure of a recombinant gap junction membrane channel.** *Science* 1999, **283**:1176-1180.

[11] Oshima A, Tani K, Hiroaki Y, Fujiyoshi Y, Sosinsky GE: **Three-dimensional structure of a human connexin26 gap junction channel reveals a plug in the vestibule.** *Proc Natl Acad Sci U S A* 2007, **104**:10034-10039.

[12] Maeda S, Nakagawa S, Suga M, Yamashita E, Oshima A, Fujiyoshi Y, Tsukihara T: **Structure of the connexin 26 gap junction channel at 3.5 A resolution.** *Nature* 2009, **458**:597-602.

[13] Oshima A, Matsuzawa T, Murata K, Tani K, Fujiyoshi Y: **Hexadecameric structure of an invertebrate gap junction channel.** *J Mol Biol* 2016, **428**:1227–1236.

[14] Bennett BC, Purdy MD, Baker KA, Acharya C, McIntire WE, Stevens RC, Zhang Q, Harris AL, Abagyan R, Yeager M: **An electrostatic mechanism for Ca2+-mediated regulation of gap junction channels.** *Nat Commun* 2016, **7**:8770.

[15] Bai XC, Yan C, Yang G, Lu P, Ma D, Sun L, Zhou R, Scheres SHW, Shi Y: **An atomic structure of human γ-secretase**. *Nature* 2015, **525**:212–217.

[16] Liao M, Cao E, Julius D, Cheng Y: **Structure of the TRPV1 ion channel determined by electron cryo-microscopy.** *Nature* 2013, **504**:107–112.

[17] Oshima A, Tani K, Fujiyoshi Y: **Atomic structure of the innexin-6 gap junction channel determined by cryo-EM.** *Nat Commun* 2016, **7**:13681 doi: 10.1038/ncomms13681.

[18] Oshima A.: **Potential of cryo-EM for high-resolution structural analysis of gap junction channels**. *Curr Opin Struct Biol* 2019, **54**:78–85

[19] Myers JB, Haddad BG, O'Neill SE, Chorev DS, Yoshioka CC, Robinson CV, Zuckerman DM, Reichow SL: **Structure of native lens connexin 46/50 intercellular channels by cryo-EM**. *Nature* 2018, **564**, 372–377.

[20] Burendei B, Shinozaki R, Watanabe M, Terada T, Tani K, Fujiyoshi Y, Oshima A: **Cryo-EM structures of undocked innexin-6 hemichannels in phospholipids.** *Sci Adv* 2020, **6**, eaax3157 doi: 10.1126/sciadv.aax3157.

[21] Oyamada M, Oyamada Y, Takamatsu T: **Regulation of connexin expression.** *Biochim Biophys Acta* 2005, **1719**:6–23

[22] Yeager M: **Structure of cardiac gap junction intercellular channels**. *J Struct Biol* 1998: **121**:231-245.

[23] Srinivas M, Costa M, Gao Y, Fort A, Fishman GI, Spray DC: **Voltage dependence of macroscopic and unitary currents of gap junction channels formed by mouse connexin50 expressed in rat neuroblastoma cells.** *J Physiol* 1999, **517**:673–689.

[24] Trexler EB, Bukauskas FF, Kronengold J, Bargiello TA, Verselis VK: **The first extracellular loop domain is a major determinant of charge selectivity in connexin46 channels.** *Biophys J* 2000, **79**:3036–3051.

[25] Suchyna TM, Nitsche JM, Chilton M, Harris AL, Veenstra RD, Nicholson BJ: **Different ionic selectivities for connexins 26 and 32 produce rectifying gap junction channels.** *Biophys J* 1999, **77**:2968–2987.

[26] Purnick PE, Oh S, Abrams CK, Verselis VK, Bargiello TA: **Reversal of the gating polarity of gap junctions by negative charge substitutions in the N-terminus of connexin 32.** *Biophys J* 2000, **79**:2403–2415.

[27] Locke D, Bian S, Li H, Harris AL: **Post-translational modifications of connexin26 revealed by mass spectrometry.** *Biochem J*. 2009, **424**:385–398.

[28] Koval M, Molina SA, Burt JM: **Mix and match: Investigating heteromeric and heterotypic gap junction channels in model systems and native tissues**. *FEBS Lett* 2014, **588**:1193–1204.

[29] Kwon T, Harris AL, Rossi A, Bargiello TA: **Molecular dynamics simulations of the Cx26 hemichannel: evaluation of structural models with Brownian dynamics.** *J Gen Physiol* 2011, **138**:475–493.

[30] Purnick PE, Benjamin DC, Verselis VK, Bargiello TA, Dowd TL: **Structure of the amino terminus of a gap junction protein.** *Arch Biochem Biophys* 2000, **381**:181–190.

[31] Kalmatsky BD, Bhagan S, Tang Q, Bargiello TA, Dowd TL: **Structural studies of the N-terminus of connexin.** *Arch Biochem Biophys* 2009, **490**:9–16.

[32] Trexler EB, Bennett MV, Bargiello TA, Verselis VK: **Voltage gating and permeation in a gap junction hemichannel.** *Proc Natl Acad Sci USA* 1996, **93**:5836–5841.

[33] Oh S, Rivkin S, Tang Q, Verselis VK, Bargiello TA: **Determinants of gating polarity of a connexin 32 hemichannel.** *Biophys J* 2004, **87**:912–928.

[34] Kasuya G, Nakane T, Yokoyama T, Jia Y, Inoue M, Watanabe K, Nakamura R, Nishizawa T, Kusakizako T, Tsutsumi A, *et al*: **Cryo-EM structures of the human volume-regulated anion channel LRRC8.** *Nat Struct Mol Biol* 2018, **25**:797–804. doi: 10.1038/s41594-018-0109-6.

[35] Kyle JW, Minogue PJ, Thomas BC, Domowicz DA, Berthoud VM, Hanck DA, Beyer EC: **An intact connexin N-terminus is required for function but not gap junction formation.** *J Cell Sci* 2008, **121**:2744–2750.

[36] Kyle JW, Berthoud VM, Kurutz J, Minogue PJ, Greenspan M, Hanck DA, Beyer EC: **The N terminus of connexin37 contains an alpha-helix that is required for channel function.** *J Biol Chem* 2009, **284**:20418–20427.

[37] Shao Q, Liu Q, Lorentz R, Gong XQ, Bai D, Shaw GS, Laird DW: **Structure and functional studies of N-terminal Cx43 mutants linked to oculodentodigital dysplasia.** *Mol Biol Cell* 2012, **23**:3312–3321.

[38] Oshima A, Tani K, Toloue MM, Hiroaki Y, Smock A, Inukai S, Cone A, Nicholson BJ, Sosinsky GE, Fujiyoshi Y: **Asymmetric configurations and N-terminal rearrangements in connexin26 gap junction channels.** *J Mol Biol* 2011, **405**:724–735.

[39] Oshima A: **Structure and closure of connexin gap junction channels.** *FEBS Lett* 2014, **588**:1230–1237.

[40] Panchin Y, Kelmanson I, Matz M, Lukyanov K, Usman N, Lukyanov S: **A ubiquitous family of putative gap junction molecules.** *Curr Biol* 2000, **10**:R473–R474.

[41] Abascal F, Zardoya R: **LRRC8 proteins share a common ancestor with pannexins, and may form hexameric channels involved in cell-cell communication.** *Bioessays* 2012, **34**:551–560.

[42] MacVicar BA, Thompson RJ: **Non-junction functions of pannexin-1 channels.** *Trends Neurosci* 2010, **33**:93–102.

[43] Deneka D, Sawicka M, Lam AKM, Paulino C, Dutzler R: **Structure of a volume-regulated anion**

channel of the LRRC8 family. *Nature* 2018, **558**:254–259.

[44] Kefauver JM, Saotome K, Dubin AE, Pallesen J, Cottrell CA, Cahalan SM, Qiu Z, Hong G, Crowley CS, Whitwam T, *et al.*: **Structure of the human volume regulated anion channel.** *Elife* 2018, **7**:e38461. doi: 10.7554/eLife.38461.

[45] Kern DM, Oh S, Hite RK, Brohawn SG: **Cryo-EM structures of the DCPIB-inhibited volume-regulated anion channel LRRC8A in lipid nanodiscs.** *ELife* 2019, **8**:e42636.

[46] Meier T, Matthey U, von Ballmoos C, Vonck J, Krug von Nidda T, Kühlbrandt W, Dimroth P: **Evidence for structural integrity in the undecameric c-rings isolated from sodium ATP synthases**. *J Mol Biol* 2003, **325**:389–397.

[47] Meier T, Matthey U, Henzen F, Dimroth P, Müller DJ: **The central plug in the reconstituted undecameric c cylinder of a bacterial ATP synthase consists of phospholipids.** *FEBS Lett.* 2001, **505**:353–356.

[48] Murata T, Yamato I, Kakinuma Y, Leslie AG, Walker JE: **Structure of the rotor of the V-Type Na+-ATPase from Enterococcus hirae.** Science 2005, **308**:654–659.

[49] Roh SH, Stam NJ, Hryc CF, Couoh-Cardel S, Pintilie G, Chiu W, Wilkens S: **The 3.5-Å cryoEM structure of nanodisc-reconstituted yeast vacuolar ATPase V_o proton channel.** *Mol Cell* 2018, **69**:993-1004.

[50] Klusch N, Murphy BJ, Mills DJ, Yildiz Ö, Kühlbrandt W: **Structural basis of proton translocation and force generation in mitochondrial ATP synthase**. *Elife* 2017, **6**:e33274.

[51] Miller AN, Long SB: **Crystal structure of the human two-pore domain potassium channel K2P1**. *Science* 2012, **335**:432–436.

[52] Brohawn SG, Campbell EB, MacKinnon R: **Physical mechanism for gating and mechanosensitivity of the human TRAAK K+ channel.** *Nature* 2014, **516**:126–130.

[53] Payandeh J, Scheuer T, Zheng N, Catterall WA: **The crystal structure of a voltage-gated sodium channel.** *Nature* 2011, **475**:353–358. doi:10.1038/nature10238.

[54] Oh S, Abrams CK, Verselis VK, Bargiello TA: **Stoichiometry of transjunctional voltage-gating**

polarity reversal by a negative charge substitution in the amino terminus of a connexin32 chimera. *J Gen Physiol* 2000, **116**:13–31.

[55] Ek-Vitorin JF, Calero G, Morley GE, Coombs W, Taffet SM, Delmar M: **pH regulation of connexin43: molecular analysis of the gating particle.** *Biophysical J* 1996, **71**:1273–1284.

[56] Henderson R, Baldwin JM, Ceska TA, Zemlin F, Beckmann E, Downing KH : **Model for the structure of bacteriorhodopsin based on high-resolution electron cryo-microscopy.** *J Mol Biol* 1990, **213**:899-929.

[57] Murata K, Mitsuoka K, Hirai T, Walz T, Agre P, Heymann JB, Engel A, Fujiyoshi Y: **Structural determinants of water permeation through aquaporin-1.** *Nature* 2000, **407**:599-605..

Annotations

20. Burendei B, Shinozaki R, Watanabe M, Terada T, Tani K, Fujiyoshi Y, Oshima A: **Cryo-EM structures of undocked innexin-6 hemichannels in phospholipids.** *Sci Adv* 2020, **6**, eaax3157 doi: 10.1126/sciadv.aax3157.

●● This work shows the first high-resolution structure of an undocked INX-6 gap junction hemichannel in a nanodisc determined by cryo-EM. The pore of the channel is blocked by double-layer densities along with N-terminal rearrangement suggesting a conformational change in the N-terminal domains in the presence and absence of phospholipids.

19. Myers JB, Haddad BG, O'Neill SE, Chorev DS, Yoshioka CC, Robinson CV, Zuckerman DM, Reichow SL: **Structure of native lens connexin 46/50 intercellular channels by cryo-EM**. *Nature* 2018, **564:**372–377.

●● The cryo-EM structures of Cx46/50 isolated from native sheep lens are reported. Intriguingly, high-resolution structure determination was achieved even though a single channel contains mixed connexins of Cx46 and Cx50. The N-terminus is reasonably oriented in the pore as hydrophobic side

chains face the pore wall.

34. Kasuya G, Nakane T, Yokoyama T, Jia Y, Inoue M, Watanabe K, Nakamura R, Nishizawa T, Kusakizako T, Tsutsumi A, *et al*: **Cryo-EM structures of the human volume-regulated anion channel LRRC8.** *Nat Struct Mol Biol* 2018, **25**:797–804. doi: 10.1038/s41594-018-0109-6.

●● This work reports a cryo-EM structure of human LRRC8A. Interestingly, a C3 hexameric channel with a different amount of space between the adjacent transmembrane bundles was determined. The asymmetric feature of compact and relaxed forms may be useful for understanding the molecular mechanism of the LRRC8A channel gating.

45. Kern DM, Oh S, Hite RK, Brohawn SG: Cryo-EM structures of the DCPIB-inhibited volume-regulated anion channel LRRC8A in lipid nanodiscs. *Elife* 2019, **8**:e42636.

● The cryo-EM structure of mouse LRRC8A in complex with DCPIB, an anionic inhibitor, in lipid nanodiscs is reported. The structure suggests a mechanism of channel inhibition by DCPIB along with lipid molecules, where DCPIB stays like a cork in a bottle. Six-fold rotational symmetry has been applied.

Figure legends

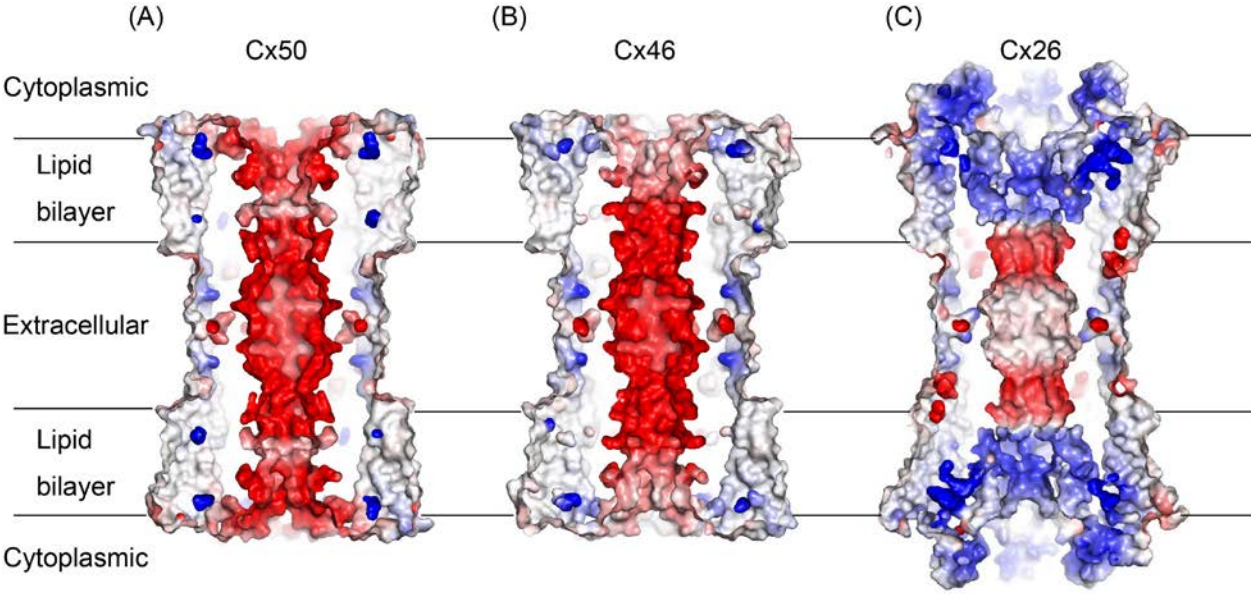

Figure 1

Electrostatic surface potential distribution of three connexin gap junction channels.

The pore surfaces of Cx50 (A) [19●●], Cx46 (B) [19●●], and Cx26 (C) [12] are shown. Negative potentials are colored in red, and positive potentials are in blue. The contour level is from –10 kT/e to +10 kT/e.

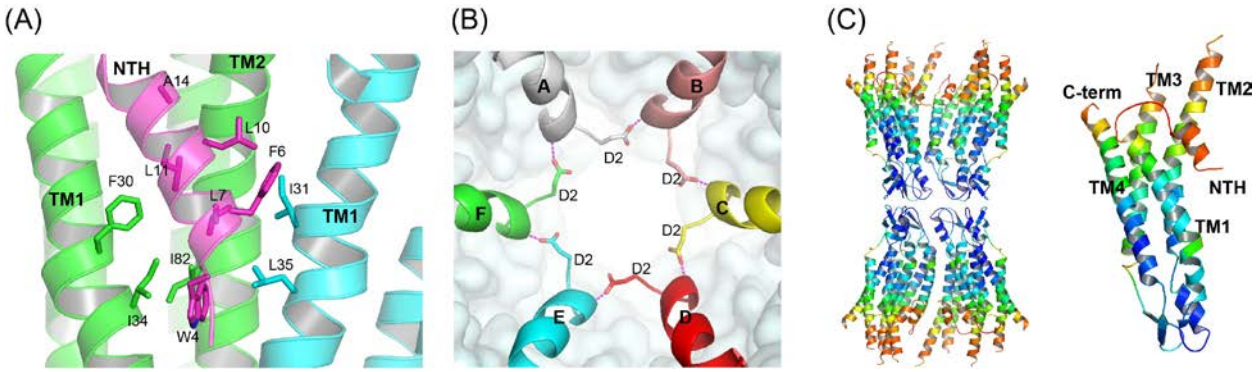

Figure 2

Structures of the N-terminal domains of Cx46 and Cx26

(A) The Cx46 pore wall viewed from inside the pore [19●●]. The N-terminal helix (NTH) of Cx46 (magenta) is distributed in the pocket generated by TM1, TM2 (green), and adjacent subunit TM1 (cyan), where the hydrophobic face of NTH is buried. The nearby hydrophobic side chains are depicted as a stick model.

(B) The X-ray structure of Cx26 shows the six NTHs forming a pore funnel stabilized by a circular network of hydrogen bonds between Asp2 and Thr5 [12]. The hydrogen bonds are shown as red dashed lines. NTH of each subunit is color coded. The pore wall of Cx26 is shown as a surface representation.

(C) Crystallographic temperature factor distribution of Cx26 [12]. A gap junction channel (left) and a monomer (right) of Cx26 are shown with colors representing the range between 70 $Å^2$ (blue) and 220 $Å^2$ (red).

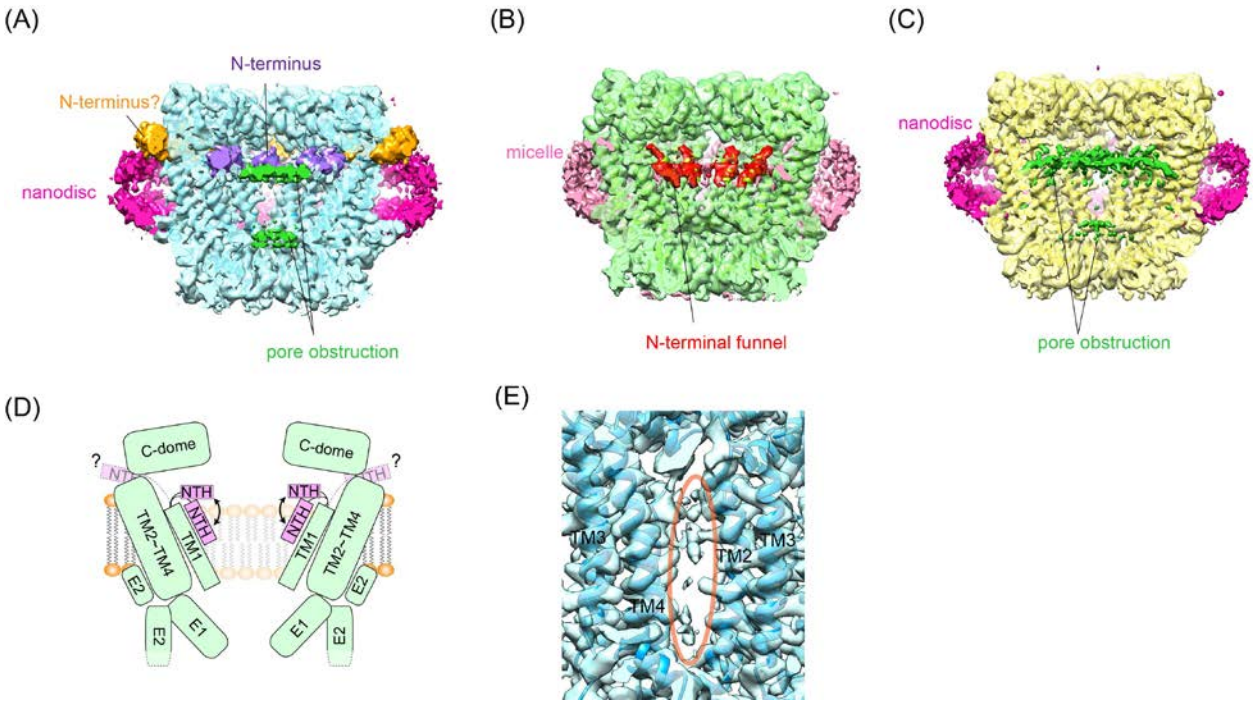

Figure 3

Cryo-EM structures of undocked INX-6 hemichannels [20●●]

(A~C) The three-dimensional structures of undocked INX-6 hemichannels of a nanodisc-reconstituted wild-type INX-6 (A), wild-type INX-6 in detergent (B), and N-terminal deleted INX-6 in a nanodisc (C). The nanodisc densities are colored in magenta, and the double-layer pore obstructing densities are shown in green. Densities, probably corresponding to the N-terminus, are shown in slate and orange, respectively. (D) Schematic representation of the N-terminal rearrangement of the INX-6 undocked hemichannel in the lipid bilayer environment. Upon reconstitution in phospholipids, the N-terminus might be deflected toward the cytoplasmic side of the channel from a funnel. It remains uncertain if the N-terminus can be deflected outside the channel. Labeling is as follows; C-dome: cytoplasmic dome, E1: first extracellular loop, E2: second extracellular loop, TM1~TM4: transmembrane helix 1 to 4, NTH: N-terminal helix. (E) Unassigned densities are observed in the space between adjacent transmembrane helix bundles (orange ellipse).